



# A New Protocol for Measuring Small Strains with a Pressuremeter Probe: Development, Design, and Initial Testing

Soufyane Aissaoui, Abdeldjalil Zadjajoui, Philippe Reiffsteck

## ► To cite this version:

Soufyane Aissaoui, Abdeldjalil Zadjajoui, Philippe Reiffsteck. A New Protocol for Measuring Small Strains with a Pressuremeter Probe: Development, Design, and Initial Testing. Measurement - Journal of the International Measurement Confederation (IMEKO), 2021, 169, 30 p. 10.1016/j.measurement.2020.108507 . hal-03575980

**HAL Id: hal-03575980**

**<https://hal.science/hal-03575980>**

Submitted on 15 Feb 2022

**HAL** is a multi-disciplinary open access archive for the deposit and dissemination of scientific research documents, whether they are published or not. The documents may come from teaching and research institutions in France or abroad, or from public or private research centers.

L'archive ouverte pluridisciplinaire **HAL**, est destinée au dépôt et à la diffusion de documents scientifiques de niveau recherche, publiés ou non, émanant des établissements d'enseignement et de recherche français ou étrangers, des laboratoires publics ou privés.

A New Protocol for Measuring Small Strains with a Pressuremeter Probe: Development, Design, and Initial Testing

Soufyane Aissaoui, Abdeldjalil Zadjiaoui, Philippe Reiffsteck

PII: S0263-2241(20)31035-6  
DOI: <https://doi.org/10.1016/j.measurement.2020.108507>  
Reference: MEASUR 108507

To appear in: *Measurement*

Received Date: 31 March 2020  
Revised Date: 2 September 2020  
Accepted Date: 21 September 2020



Please cite this article as: S. Aissaoui, A. Zadjiaoui, P. Reiffsteck, A New Protocol for Measuring Small Strains with a Pressuremeter Probe: Development, Design, and Initial Testing, *Measurement* (2020), doi: <https://doi.org/10.1016/j.measurement.2020.108507>

This is a PDF file of an article that has undergone enhancements after acceptance, such as the addition of a cover page and metadata, and formatting for readability, but it is not yet the definitive version of record. This version will undergo additional copyediting, typesetting and review before it is published in its final form, but we are providing this version to give early visibility of the article. Please note that, during the production process, errors may be discovered which could affect the content, and all legal disclaimers that apply to the journal pertain.

# A New Protocol for Measuring Small Strains with a Pressuremeter Probe: Development, Design, and Initial Testing

Soufyane AISSAOUI<sup>1</sup>, Abdeldjalil ZADJAOU<sup>2</sup>, Philippe REIFFSTECK<sup>3</sup>

<sup>1</sup>PhD Student, Department of Civil Engineering, Faculty of Technology, University Aboubekr BELKAID, Tlemcen, 22 rue Abi Ayed Abdelkrim, Fg Pasteur BP 119. 13000, Algeria. E-mail: aissaouisoufyane@yahoo.fr

<sup>2</sup>Professor, Department of Civil Engineering, Faculty of Technology, University Aboubekr BELKAID, Tlemcen, 22 rue Abi Ayed Abdelkrim, Fg Pasteur BP 119. 13000, Algeria. E-mail: a.zadjaoui@gmail.com

<sup>3</sup>Professor, Geotechnical Engineering, Environment, Natural Hazards and Earth Sciences Department, French Institute of Science and Technology for Transport, Development and Networks (IFSTTAR), University of Paris-Est, Champs sur Marne F-77447, Marne la Vallée Cedex 2, France. E-mail: philippe.reiffsteck@ifsttar.fr

## Abstract

Soil characterization plays a key role in the construction of various civil engineering infrastructures. For the purpose of developing a geotechnical design model, it is essential first to describe the behavior of natural soil masses before proceeding to the calculation of a structure. The use of numerical modeling for solving soil-structure interaction problems is a crucial prerequisite; these problems can be solved properly just by measurement of small-strain stiffness and the stiffness degradation curve of soils. To meet these needs, the present paper starts by introducing the concept of a new pressuremeter probe equipped with a Hall Effect sensor that provides reliable small strain measurements of the mechanical properties of soils. The main steps that allowed validating of the new pressuremeter probe and the results obtained from previous tests in a physical model are presented in the second part. This approach allows drawing a degradation curve of the shear modulus; this would be useful in the practice of geotechnical engineering, and particularly for a better understanding of the nonlinear behavior of soils subjected to dynamic or seismic loads.

**Keywords** - Design; Pressuremeter; Small Strains; HALL Effect; Calibration; Validation.

## 1. INTRODUCTION

Control of deformations of soils and structures as well as their interactions, especially in urban areas, plays an increasingly important role in geotechnical studies (Mestat and Reiffsteck, 2002). The control process assumes a reliable and relevant estimation of soil deformability characteristics (Mair and Wood, 1987). Soil mechanical parameters can be determined in the laboratory on specimens collected from the field, or directly in situ by means of expansion or penetration tests (Kaggwa et al., 1996). Currently, in situ tests are preferred by practitioners and are routinely performed in geotechnical engineering (Schnaid, 2006). Unlike those carried out in the laboratory, these tests have the advantage of not requiring a sampling step, and therefore the results obtained are not likely to suffer from any distortion that may result from a possible disturbance. On the other hand, these tests do not allow for a complete control of the test conditions, and consequently some information that could be provided by the laboratory test may be missed (Clayton, 2011).

Recent developments in civil engineering have created multiple problems of interaction between structures and soils, particularly when building large structures in cities and their subsoils (Borel and Reiffsteck, 2006); these are essentially problems of compatibility of deformations that can only be reliably handled by knowing the deformability of the different soils at low strain levels. In order to directly control the deformations of soils and structures as well as their interactions, a lot of research has been carried out for the purpose of developing new in-situ soil monitoring devices such as the penetrometers, dilatometers and pressuremeters, which have previously been discussed in the works of Garneau and Samson (1974), Thorel et al. (2007), Cui (2011), Qiao (2011), Shaban and Cosentino (2017), etc. These devices were developed for a better knowledge of soil parameters, and also for the development of a method which makes it possible to deduce useful data that can actually be used in controls, calculations and regulatory justification of the geotechnical structures.

The present study concentrates on the pressuremeter, a device commonly used today in most geotechnical engineering projects in a number of countries, especially in foundation projects (Baguelin et al., 1978; Amar et al., 1991). The pressuremeter test, which was invented by Kögler in the thirties (Kögler, 1933), was later fully developed at the instigation of Ménard (1955). This test is a comprehensive tool that uses various structural design methods (shallow foundations, deep foundations, retaining walls, etc.). According to one aspect of the invention, the principle of in-situ experimentation consists of introducing a diametrically deformable cylindrical cell into a borehole at staggered depth values. The diameter of the cell must fit into the borehole, but without proper elastic reaction. Next, the cell is inflated with an incompressible fluid on demand and according to a well-defined pressure-time program. The pressuremeter test was standardized by the end of the 60's, and its current operating mode is specified in the French standard EN ISO 22476-4 (2005) and American standard D 4719 (ASTM, 2007).

For their part, Johnston et al. (2013), Wang et al. (2018), and Masoud & Khan (2019) made an attempt to improve the measurement of soil deformability by eliminating soil remolding due to borehole creation. The probes were equipped with local measurement transducers.

The present paper is intended to investigate the problem mentioned above. Indeed, it seeks to develop a new pressuremeter apparatus (a probe) that helps practitioners to have richer information concerning small-strain stiffness. This new apparatus is particularly supplied with a measuring feeler located at its center in order to determine the initial shear moduli. The methodology, apparatus calibration and validation of results are also provided.

## **2. REVIEW OF PREVIOUS WORK**

### **2.1. *Practical interest of small strain measurement***

According to Likitlersuang et al. (2013), it is highly important to know the mechanical parameters of soil, such as the deformation modulus, as well as their evolution from small to large strains; it is also essential to determine their variation along the stress path as a function of the applied load. Moreover, it is worth mentioning that each test has a field of application corresponding to the generated soil

deformations. These deformations must be related to those that appear during the realization or the exploitation of the structures (Burland, 1989).

The measured deformation moduli depend on the type of equipment and procedure used, as well as on the strain range tested. Figure 1 displays the various domains where this laboratory equipment is commonly used (Atkinson and Salfors, 1991; Mair, 1993) as well as their application ranges (Tatsuoka et al., 1997; Reiffsteck, 2002) for the determination of the deformation moduli.

From a practical point of view, Atkinson and Salfors (1991) considered three strain ranges for soils. The first one has to do with very small strains (less than 0.001%), where the shear modulus  $G$  varies very little around a maximum value  $G_{max}$ . The second one relates to small strains (between 0.001% to 1%); here the  $G$  modulus varies non-linearly with the strain. The third one is for large strains that go with strains greater than 1% ( $1 \cdot 10^{-2}$ ); in this case, the soil approaches rupture and the shear modulus is very low.

Knowledge of the behaviour of soils under small strains is an important step in understanding the complex status of the soil surrounding civil engineering structures such as retaining walls, foundations or tunnels. This is particularly important in the field of road construction where the stresses due to vehicles affect the behavior and the lifetime of a road structure. Similarly, the geotechnician must pay attention to small strains that could be caused by an earthquake; this can bring about changes in the soil-structure interactions (Jardine et al., 1986; Benz et al., 2009; Oztoprak and Bolton, 2013). Determination of the shear modulus at small strains presents a big challenge for the calculation of structures, especially when the deformation methods or dynamic computations are used (Zhang et al., 2005; Vardanega and Bolton, 2013).

These observations reveal a need to know the behaviour of soils under small strains that may appear under exceptional loading or seismic solicitations. In addition, the experiments and tests must be performed with accurate and sophisticated equipment.

## **2.2. Small strain measurements**

Various methods for laboratory and in-situ measurements of small strains have been developed over the past thirty years. Furthermore, two main techniques deserve citation, namely the quasi-static method and the dynamic method.

Various types of sensors have been developed for the quasi-static technique. For instance, Burland and Symes (1982) developed a displacement sensor, which was in fact an inclinometer that allows measuring both the axial and radial strains. Afterwards, many measurement devices based on other principles were developed. In addition, Clayton & Khattrush (1986) and Clayton et al. (1989) developed a Hall Effect displacement sensor to evaluate the small strains of the order of  $2 \cdot 10^{-5}$ . As for Gotto et al. (1991), they developed the local deformation transducer (LDT) to measure local strains of the order of  $10^{-6}$ . Also, Cuccovilo & Coop (1997) proposed the use of the linear variable differential transformer

(LVDT) which is a submersible device that helps to measure local axial and radial strains up to the value  $10^{-6}$ . Unlike the quasi-static methods, the dynamic methods involve sufficiently high variations in deformation velocity so that the inertial forces are non-negligible in the fundamental laws of dynamics. These methods may involve stationary wave propagation or not: geophones (Modoni et al., 1999), bender elements (Jovicic et al., 1996; Kuwano et al., 1999; Fioravante, 2000; Gu et al., 2013), resonant columns (Cascante and Santamarina, 1997; Tatsuoka et al., 1997).

With regards to in situ tests, the progress achieved was not so spectacular because the measurements of very small strains were difficult to perform and were conducted under hard field conditions inside boreholes due to the disturbing effects of positioning the apparatus and the anisotropy of natural environment. Note that there are some geophysical methods, i.e. the cross hole test (Stokoe and Woods, 1972) and the downhole test (Woods, 1978), that are based on shear wave propagation, but unfortunately they are valid only in the range of very low strain rates ( $10^{-7}$  to  $10^{-6}$ ) and for a homogeneous ground mass. In addition, it is interesting to mention that there are devices, like self-boring pressuremeters, that are capable of measuring the soil stiffness under small strains. For instance, the self-boring pressuremeter was initially developed by Jézéquel and Touzé (1970) in conjunction with Wroth and Hughes (1972), and was subsequently improved by other researchers (Withers et al., 1986; Fahey and Jewell, 1990; Campanella et al., 1990; Clarke and Smith, 1992; Akbar, 2001; Reiffsteck et al., 2005; Rehman, 2010). Note that this pressuremeter is still expensive and needs highly skilled operators.

### 3. APPARATUS - DEVELOPMENT AND DESIGN

#### 3.1. Probe design

Figure 2 presents the schematic diagram of the conceptual design of the proposed probe. A standard Ménard probe, 60 mm in diameter, consisting of three cylindrical cells of circular section with the same axis was used (EN ISO 22476-4, 2005). The geometric characteristics of the probe are given in Table 1.

As clearly shown in Figure 3, a test plate was inserted inside the central measuring cell. A portion of the standard probe was cut off and then a new measuring system was inserted.

The zone cut at the central measuring cell is illustrated in Figure 4. This zone is waterproof, which makes it possible to preserve water and gas; a 150 mm long slot was made in the middle of the probe in order to take measurements at the midpoint of the membrane. The inner diameter of the probe, at the level of the central cell, is 41.5 mm. This probe was cut to a depth of  $h = 25$  mm, as illustrated in Figure 4. This distance was chosen for installation of the measurement system in an easy and convenient way.

Figure 5 illustrates a schematic representation of the first prototype; it also shows how the measurement zone is created in the central cell.

### **3.2. Deformation measurement system**

In contrast to the conventional method, the developed pressuremeter uses a pneumatic system rather than a hydraulic system. That is, cell pressure is applied by way of nitrogen gas-filled membrane and displacements are measured directly using a measuring feeler, rather than inferring displacements from measured volume changes. It is believed that the direct measurement of cavity strain removes a number of potential sources of error inherent in the inference of displacement from the volume change.

The measuring feeler is made of high strength stainless steel (36NiCrMo16). It consists of two arms and a support for the Hall Effect sensor. At the initial position (no expansion of the membrane), the distance between the outer ends of the two arms (upper and lower) of the measuring feeler (expansion arms) is equal to the inside diameter of the probe (i.e. 41.5 mm) as shown in Figure 6. The arms can move radially from 41.5 mm to a maximum of 71.5 mm.

The Hall Effect sensor was positioned on a suitable support placed between the two arm magnets. The dimensions of the sensor seat allow covering a measuring range of about 30 mm, as shown in Figure 6 b. which corresponds to the maximum limit that the device can reach, i.e. when the portion carrying the second magnet comes into contact with the support of the Hall Effect sensor.

A present limitation of Ménard type pressuremeter test is due to the difficulty of reaching large expansion volumes and high pressures without exposing to significant risks of bursting. The expansion measurement system in the developed pressuremeter can record the cavity strain to about 72% of its original size, which is more than the minimum (50%) specified by Withers et al. (1986) and Clarke (1997). The new pressuremeter allowing the volume of the hole to be doubled, even under high pressures: the conventional limit pressure can then be directly measured.

The data acquisition system was placed at floor level; it is connected to the different sensors through cables. It allows acquiring and recording all data obtained from the pressuremeter test.

## **4. CALIBRATION OF THE MEASUREMENT SYSTEM**

Proper sensor calibration was carried out to allow converting the analog output into pressure and radial expansion units during an expansion test. Moreover, this operation ensures the correct operation of the equipment (reliability, productivity and representativeness). The equipment includes the Hall Effect sensor with its measurement scheme and the pressure sensor.

### **4.1. Calibration procedure of the displacement sensor**

The primary purpose for using this type of Hall Effect sensor is to allow for the measurement of radial displacements without contact. According to Asch (2010); Clayton et al. (1989), the Hall Effect was employed in a device developed by Clayton and Khatrush (1986) for measuring local axial strains on triaxial specimens. These same authors indicated that “if a metallic or semiconductor plate traversed by a current is placed in a magnetic field with flux lines directed perpendicularly to the plate and the current flow, then the charge carriers (i.e., electrons) will be deflected so that a voltage is produced across the plate in a direction normal to the current flow. This voltage is known as the Hall voltage.



The sensor was supplied with a DC voltage with a power source of 15 volts on one of the terminals marked +; another one marked - was connected to the ground, and the third one noted 0, which uses the ground as reference, was used for measurements (Figure 7). The Hall Effect sensor is connected to the analog digital converter (A/D NI usb-6000 box) at the surface using an electrical cable.

Calibration of the radial movement of the arms against the variation of the output voltage of the sensor was carried out before installing the membrane on the probe. This allows determining the relationship between the voltage generated by the sensor, and recorded by a National Instruments data acquisition system, and the radial movement of the measuring feeler arms. The probe was fixed in a horizontal position with all the parts needed for the calibration operation. Then, a digital Vernier caliper was used to measure the relative movement of the arm; the measurements were performed every millimeter until the arm reaches the maximal position of 30 mm. It is worth noting that the procedure was performed on a single arm of the measuring feeler, while the other one remained fixed.

Calibration was initially performed by means of two different analog sensors of references SS94A1F and SS94A2 for the purpose of highlighting the effect of sensor type on the results. The difference between the two sensors lies in the measurable magnetic field intensity range. Indeed, sensor SS94A1F measures the values within the range  $[-100, +100]$  Gauss, while sensor SS94A2 measures values within the interval  $[-500, +500]$  Gauss. This is explicitly shown in Figure 8. Sensor SS94A1F cannot adequately cover the entire measurement range because the magnetic field cannot be fully detected. It seems that it can be detected in a range that is limited to a displacement equal to about 18 mm. Figure 8 suggests that the uniqueness of the answer is compromised. The same voltage reading can be obtained for two different displacement values, and consequently, this sensor can be discarded. On the other hand, it was found that sensor SS94A2 covers a larger displacement range that corresponds to the trajectory of the measuring feeler. The measured voltage corresponds to the recorded movement. It is important that this displacement does not exceed 30 mm. This result is consistent with reality. Therefore, the SS94A2 sensor can be retained for future use.

Unfortunately, it turned out that the pressuremeter test results obtained after the sensor calibration do not seem to be consistent with the overall appearance of the standard Ménard curve, indicating that there is a calibration problem. Figure 8 showing that the relationship between displacement and output voltage is approximately linear in the volts = 1 ~ 1.2v, since in this range we are very close to the magnetic field created by the magnet of the measuring feeler arm. As the magnetic field increases around the Hall Effect sensor, a better linearization in its response is obtained. Beyond the measuring range of 4mm, we notice immediately that the response of the Hall Effect sensor presents a non-linearity which is justified by the decrease of the magnetic field around the sensor. To remediate this problem, another series of tests was carried out while increasing the diameter of the magnet, at the same position, but the results were still



unacceptable. For this, it was envisaged to extend the magnetic field by adding another magnet in the lower part of the same arm.

Furthermore, it was found that the variation in the response of the Hall Effect sensor as a function of magnetic polarization was very high. Accordingly, two tests were carried out: 1) The first one with a single magnet and 2) The second one with two magnets. The double polarization contribution can clearly be observed in Figure 9. The case where two magnets are used seems to be more realistic as it approaches the linearization of the response, which is an encouraging result. It is noted at this level that the affixed orientation of the two magnets (N-S, S-N) contributes favorably to the linearization of the response. It is worth noting from Figure 9 that the case where two magnets are used provides more accuracy, which is our main objective.

Subsequently, two magnets were used; one at the top and the other at the bottom of the arm.

#### **4.2. Calibration of the pressure sensor**

The applied pneumatic pressure is controlled using a Jean Lutz controller device and associated software package which allows the pressure to be varied precisely and at a specified rate. The objective was to achieve a good accuracy essentially in the measurements of the pressure applied to the probe. For this, the applied gas pressure was measured using a gas pressure sensor (KELLER, the manufacturer) located in the Jean Lutz controller device, whose role was to acquire the pressure value and transmit it to the new digital indicator EV-06, as shown in Figure 10.

The calibration results are summarized in Figure 11, along with the equation obtained through linear regression. Note that there is a rapid and substantially linear variation in voltage as a function of the applied pressure. The test was repeated three times, and the results obtained seemed consistent. As can be seen on the calibration curve, the abscissa at the origin, i.e. the indication given for a zero pressure, is equal to 0.08 V which corresponds to the atmospheric pressure.

### **5. RESULTS AND INTERPRETATION**

The experimental program consists of performing a series of validation tests in order to determine the main limitations of the developed equipment and check its performance. To achieve this, multiple tests were conducted using a simple physical model. For experimental reasons (simplicity, control, homogeneity), it was decided to place a sandy soil sample of known behaviour and characteristics into a metal tank in such a way that the sample simulates the real conditions of the test (Figure 12). Though these tests were carried out in the laboratory, it was still possible to analyze and assess the power, quality, performance as well as the shortcomings of our equipment. Based on the results obtained, it was possible to identify the strain range that can be explored by this probe.

The tank used is a barrel 90 cm high and 60 cm in diameter. Coarse sand brought from the Seine River was pluviated to achieve a homogenous fixed relative density. The characteristics of sand used are summarized in Table 2. Figure 13 presents the grain size distribution curve of the Seine River sand.

For the tests performed in laboratory calibration chamber on soil specimens of reference Seine River sand. The new probe is carefully jacked into the ground in such a way that there is little or no disturbance caused to the surrounding soil, the initial pressuremeter pressure corresponding to zero cavity strain should theoretically be equal to the in-situ total horizontal stress ( $\sigma_{h0}$ ). In the in-situ tests, as a predrilled borehole is required for the installation of the instrument, severe disturbance is induced in the surrounding soil. The first portion of the expansion curve shows the pressure that must be applied to push the membrane into contact with the soil ( $\sigma_{h0}$ ). The knowledge of this contact pressure value, allows us to subtract this contact pressure part from the total soil response. This allows us to know with precision the values of the small strain range of the soils.

At first, the monotonic tests were carried out in a tank of loose sand with identical pressure increments of about 10 kPa; it should be noted that each pressure had to be maintained for a period of 60 s, in accordance with standard EN ISO 22476-4 (2005).

For each test, the applied pressure ( $p_r$ ) and the membrane displacement ( $\Delta R$ ) during the expansion were recorded in real time. The results of the monotonic tests (raw and corrected curves) are first presented, followed by the degradation of the derived shear modulus.

A calibration test was carried out before performing all monotonic tests in order to check the membrane rigidity. Figure 14 shows the membrane resistance curve  $p_e(\varepsilon_r)$  at  $t = 1s$  and  $t = 60s$ . This same figure presents also the double hyperbolic curve that represents the shape of the calibration curve. The value of the corrected pressure ( $p_c$ ) can be obtained directly from the following expression:

$$p_c = p_r - p_e(\varepsilon_r) \text{ with } \varepsilon_r = \frac{\Delta R}{R_0} \quad (1)$$

Note that  $p_c$  is the corrected pressure,  $p_r$  the raw pressure,  $p_e$  the pressure due to the resistance of the membrane,  $\varepsilon_r$  the radial strain,  $\Delta R$  the variation of the radius of the cavity, and  $R_0$  the initial radius of the cavity.

The correction is given by the expression of the double hyperbolic curve given below:

$$p = A_1 + A_2 * \varepsilon_r + \frac{A_3}{A_5 - \varepsilon_r} + \frac{A_4}{A_6 - \varepsilon_r} \quad (2)$$

An iterative process was performed using the Microsoft Excel spreadsheet to obtain the parameters  $A_i$  ( $i = 1$  to 6) connecting the corrected pressure ( $p_c$ ) to the radial deformation ( $\varepsilon_r$ ).

There are six parameters:

$$A_1 = 2,495626 \quad A_2 = 0,052684 \quad A_3 = 0,0023743 \quad A_4 = -227,41643 \quad A_5 = -0,01043 \quad A_6 = 99,82631$$

The correlation between the relative density and resistance to dynamic penetration was used in order to find the sand density. It is obvious that if the results of the different tests give the same dynamic resistance, it means that this should also be true for the density.

Penetrometer tests with PANDA 3® Labo (Dynamic Digital Autonomous penetrometer) were carried out before each test with the developed pressuremeter. The objective was to formulate soil test pieces that guarantee the homogeneity of the relative density (the test pieces have constant relative density). The relative density is an important quantity for the rigorous control of relevance, feasibility and repeatability of the developed apparatus.

The penetrograms obtained in Figure 15 show, at first sight, that the soil used in the laboratory is of relatively good quality, which indicates that it has a good homogeneity since the peak resistance values are practically identical. The above-mentioned findings indicate therefore that the homogeneity factor is ensured for all the pressuremeter tests performed on loose sands.

Figure 16 shows all monotonic tests performed on loose sand. One can see that the tests were repeated a certain number of times. The repeatability of tests confirms the importance of the measurements performed and their accuracy.

The data obtained from Figure 16 show a good consistency with the results of the expansion tests, in the case of monotonous loading. No problem of repeatability arose during the entire experimental planning. At this point, it can be said that the fabricated probe is functional.

The pressuremeter curve is a stress strain curve where the stress is the measured pressure and the strain is the hoop strain  $\varepsilon_r$ . It is therefore possible to define a shear modulus as a function of strain from the pressuremeter curve; the shear modulus degradation is clearly displayed in Figure 17. This modulus can be directly calculated from the pressuremeter curve, at different strain level, with the following equation:

$$G = \frac{1\Delta p}{2\varepsilon_r} \quad (3)$$

The shear modulus obtained from equation 3 for any radial stress strain level allows to derive the shear modulus degradation characteristics. Figure 17 shows how the shear modulus degradation took place during tests 2, 3, 4 and 6. For example, one can easily observe the low shear modulus values measured in loose sand. In addition, a good correlation is noted between the strain zone under consideration and the type of soil tested. Consequently, it can be said that for the same type of test, the modulus values increase when the strain of the edge of the cavity decreases.

Based on the analysis of previous tests, it was possible to make an assumption that seems acceptable concerning continuous loading at a constant load rate of 2 kPa/s with data recorded at every second; the

objective sought was to accurately analyze the gain on the shear modulus by considering a larger number of points.

Measurements under small strains can be significantly improved. This may be done through gradual loading of the ground by a constant bearing pressure until maximum displacement of the measuring feeler is reached. The results of these tests are presented in Figure 18.

In a similar way, the degradation of the shear modulus for this continuous loading can be evaluated every second. Figure 19 clearly shows the evolution of this degradation as a function of strain. A double contribution of the hypothesis was made at the beginning of this paragraph: 1) The amplitude of measured moduli is greater than that of the standardized loading; 2) The measurement zone of small strains is larger. Note that the duration of the continuous loading test is almost four times greater than that of a standard loading. This procedure responds more rigorously to the objectives of being able to access small strains.

Once again, in order to meet the objective of measuring small strains, a series of tests were conducted on dense sand. The purpose of the procedure is two-fold: 1) First to test the good functioning of the probe, and 2) Second, to identify the measurement range limits of that probe.

After complete saturation, heavy compaction by suitable compacting equipment was initiated. An attempt was made to produce maximum compaction for the four tests to be performed. Figure 20 displays the results recorded from the tests (raw curves), and those obtained after correction (corrected curves).

Figure 21 depicts the semi-logarithmic curves representing the evolution of shear modulus of dense sand (tests 1 to 4) as a function of radial strain. This evolution is similar to those reported by Atkinson and Salfors (1991), and Tatsuoka et al. (1997).

This figure allows drawing the following conclusions:

- ❖ The variation of  $G$  as a function of radial strain is strongly non-linear, and the shear modulus depends on stresses and strains.
- ❖ There is a small strain domain for which the shear modulus has a maximum value of about 90 MPa around a strain of  $10^{-4}$ . After that value, this modulus starts decreasing to reach its minimum zero value where the soil is approaching rupture
- ❖ Finally, it is worth noting that the shear modulus of a material is a parameter that depends not only, as we have seen before, on the level of strain at which the measurement takes place, but also on the density of soil.

To compare the shear modulus values obtained, it was decided to perform classic Ménard tests in the chamber (loose state). As depicted in Figure 22, the maximum shear modulus value, calculated by the developed probe (PRSMOD), is equal to 25 bars; it is 4 to 5 times greater than the value recorded by the conventional Ménard probe. This result confirms the impact of strain rate (about  $10^{-3}$  for the developed probe and around  $10^{-1}$  for the conventional probe) on shear modulus. Consequently, it might be concluded that the new probe allows recording a broader range of strain values, which is in full agreement with the purpose of the present study.

The probe developed in this work makes it possible to assess the shear modulus at a strain rate that corresponds to what is generated by an earthquake ( $10^{-3}$ - $10^{-2}$ ), whereas the classic Ménard probe remains limited to the interval  $10^{-2}$ - $10^{-1}$ . Improvements are still needed to reach the range  $10^{-4}$ - $10^{-3}$ .

Though these tests were carried out in the laboratory, it was possible to analyze the power, quality, performance of the device developed here. These also allowed identifying its limitations and shortcomings. The above findings support the fact that the developed probe can reproduce the non-linear behavior of soils. In this case, the definition of the shear modulus is relevant for the design of geotechnical structures.

## 6. CONCLUSIONS

This paper explains in detail the design, manufacture and operation of a new pressuremeter probe that is used to measure deformability properties of soil, and more particularly its shear or deformation modulus.

This study is a major contribution to better understanding small strain behaviour of soils under seismic loading. The probe developed in this study is different from the conventional Ménard pressuremeter ; indeed, this is a system that can measure the radial strain of the membrane as it uses a measuring feeler equipped with a Hall Effect sensor instead of deducing the strain from the measurement of the variations of the volume of a fluid.

Experiments were conducted in the laboratory on an artificial soil consisting of sand from the Seine River, in loose and dense states. The results of the tests conducted with the developed pressuremeter allow confirming the feasibility of the tests, their reproducibility and mainly the degree of accuracy of the device. Satisfactory and relevant values of the shear modulus could be obtained at small strain levels.

This new pressuremeter can also help to characterize soils and to determine the shear modulus degradation within intervals extending from low to medium strain rates. For a more exhaustive validation, it would be interesting to test this pressuremeter probe in clay-loam soils as well.

## References

- Akbar A. (2001).** Development of low cost in-situ testing devices. PhD thesis of doctor of philosophy, Newcastle-upon tyne University, 369 pages.
- Amar S., Clarke B.G., Gambin M.P., Orr T.L.L. (1991).** The application of pressuremeter test results to foundation design in Europe. European Regional Technical Committee N°. 4, Pressuremeters, Edition Balkema A.A, Ed., pp. 1-24.
- Asch G. (2010).** Les capteurs en instrumentation industrielle. Ed Dunod, 7<sup>ème</sup> edition, 864 pages.
- ASTM D4719 (2007).** Standard Test Method for Prebored Pressuremeter Testing in Soils. annual book of ASTM standards, Section 4, v. 04.08.
- Atkinson J.H., Sallfors G. (1991).** Experimental determination of stress-strain-time characteristics in laboratory and in-situ tests. Proc. 10<sup>th</sup> Euro. Conf. Soil Mechanics and Foundation Engineering, Florence, pp. 915-956.
- Baguelin F., Jézéquel J.F., Shields D.H. (1978).** The pressuremeter and foundation engineering. Transtech publications, 618 pages.
- Benz T., Schwab R. Vermeer P. (2009).** Small-strain stiffness in geotechnical analyses. Bautechnik special issue, pp. 16-27
- Borel S., Reiffsteck Ph. (2006).** Caractérisation de la déformabilité des sols au moyen d'essais en place. Etudes et recherches des laboratoires des ponts et chaussées, série géotechnique, 132 pages.
- Burland J.B. (1989).** Ninth Laurits Bjerrum memorial lecture : « Small is beautiful » the stiffness of soils at small strains. Canadian Geotechnical Journal, vol. 26, N°. 4, pp. 499-516. <https://doi.org/10.1139/t89-064>
- Burland J.B., Symes M.J. (1982).** A simple axial displacement gauge for use in triaxial apparatus. Geotechnique, Vol. 32, N°. 1, pp. 62-65. <https://doi.org/10.1680/geot.1982.32.1.62>
- Campanella R.G., Stewart W.P., Jackson R.S. (1990).** Development of the UBC self-boring pressuremeter. Proceeding of the 3rd International Symposium on Pressuremeter, organised by the British geotechnical society and held at Oxford university, pp. 65-73.
- Cascante G., Santamaria C. (1997).** Low strain measurements using random noise excitation. Geotechnical Testing Journal, Vol. 20, N°. 1, pp. 29-39. <https://doi.org/10.1520/GTJ11418J>
- Clarke B.G. (1997).** Pressuremeter Testing in Ground Investigation, Part II-Interpretation. Proceedings of the Institution of Civil Engineers - Geotechnical Engineering, pp 42-52. <https://doi.org/10.1680/igeng.1997.28996>
- Clarke B.G., Smith A. (1992).** Self-boring pressuremeter test in weak rocks. Construction and building materials, Vol. 6, N°. 2, pp. 91-96. [https://doi.org/10.1016/0950-0618\(92\)90057-6](https://doi.org/10.1016/0950-0618(92)90057-6)
- Clayton C.R.I. (2011).** Stiffness at small strain : research and practice. Géotechnique, Vol. 61, N°. 1, pp. 5–37. <https://doi.org/10.1680/geot.2011.61.1.5>
- Clayton C.R.I., Khatrush S.A (1986).** A new device for measuring local axial strains on triaxial specimens. Géotechnique, Vol. 36, N°. 4, pp. 593-597. <https://doi.org/10.1680/geot.1987.37.3.413>
- Clayton C.R.I., Khatrush S.A., Bica A.V.D., Siddique A. (1989).** The use of Hall effect semiconductors in geotechnical instrumentation. Geotechnical Testing Journal, ASTM, Vol. 12, N°. 1, pp. 69-76. <https://doi.org/10.1520/GTJ10676J>.
- Cuccovillo T., Coop M.R. (1997).** The measurement of local axial strains in triaxial test using LVDTs. Géotechnique, Vol. 47, N°. 1, pp. 167–171. <https://doi.org/10.1680/geot.1997.47.1.167>
- Cui X. (2011).** Development of Electronic Miniature Cone Penetrometer and Penetration Test in Silty Clay. Geotechnical Special Publication, pp. 108-115. [https://doi.org/10.1061/47626\(405\)14](https://doi.org/10.1061/47626(405)14)
- EN ISO 22476-4. (2005).** Geotechnical investigation and testing – Field testing. Part 4 : Ménard pressuremeter test. Projet de norme CEN/TC341 WG5.
- Fahey M., Jewell R.J. (1990).** Effect of pressuremeter compliance on measurement of shear modulus. Proceedings of the Third International Symposium on Pressuremeters, organised by the British Geotechnical Society and held at Oxford University, pp. 115-124.
- Fioravante V. (2000).** Anisotropy of small strain stiffness of Ticino and Kenya sands from seismic wave propagation measured in triaxial testing. Soils and Foundations 40 (4), pp. 129-142. [https://doi.org/10.3208/sandf.40.4\\_129](https://doi.org/10.3208/sandf.40.4_129)
- Garneau R., Samson L. (1974).** A Device for the Constant Rate of Penetration Test for Piles. Canadian Geotechnical Journal, Vol.11, No.2, pp. 298–302. <https://doi.org/10.1139/t74-025>



- Goto S., Tatsuoka F., Shibuya S., Kim Y.S., Sato T. (1991).** A simple gauge for local small strain measurements in the laboratory. *Soils and foundations*, Vol. 31, N° 1, pp. 169-180. <https://doi.org/10.3208/sandf1972.31.169>
- Gu X., Yang J., Huang M. (2013).** Laboratory measurements of small strain properties of dry sands by bender element. *Soils and Foundations*, vol.53, No. 5, pp. 735-745. <https://doi.org/10.1016/j.sandf.2013.08.011>
- Jardine R.J., Potts D.M., Fourie A. B., Burland J. B. (1986).** Studies of the influence of non-linear stress-strain characteristics in soil-structure interaction. *Géotechnique*, Vol. 36, N° 3, pp. 377-396. <https://doi.org/10.1680/geot.1986.36.3.377>
- Jézéquel J.F., Touzé J. (1970).** Sonde foreuse pressiométrique. Brevet d'invention N°. 1.596.747, 5 pages.
- Johnston G., Doherty J., Lehane B. (2013).** Development of a laboratory-scale pressuremeter. *International Journal of Physical Modelling in Geotechnics* Vol.13, N01, pp. 31–37. <https://doi.org/10.1680/ijpmg.12.00011>
- Jovicic V., Coop M.R., Simic m. (1996).** Objective criteria for determining Gmax from bender element (technical note). *Géotechnique*, Vol. 46, N°. 2, pp. 357-362. <https://doi.org/10.1680/geot.1996.46.2.357>
- Kaggwa W.S., Jaksa M.B., Jha R.K. (1996).** Development of automated dilatometer and comparison with cone penetration tests at the University of Adelaide. Australia, *Advances in Site Investigation Practice*, London; pp. 372-382.
- Kögler F. (1933).** Baugrunprüfung im Borloch. *Der Bauingenieur*, Berlin Heft N°. 19/20.
- Kuwano R., Connolly T.M., Kuwano J. (1999).** Shear stiffness anisotropy measured by multi-directional bender element transducers. *Pre-failure Deformation Characteristics of Geomaterials*, Rotterdam : Balkema, pp. 205-212.
- Likitlersuang S., Teachavorasinskun S., Surarak C., Oh E., Balasubramaniam A. (2013).** Small strain stiffness and stiffness degradation curve of Bangkok Clays. *Soils and foundations*, Volume 53, N°. 4, pp. 498-509. <https://doi.org/10.1016/j.sandf.2013.06.003>
- Mair R.J. (1993).** Unwin memorial lecture 1992. Developments in geotechnical engineering research: application to tunnels and deep excavation. *Proceedings of the ICE-Civil Engineering*, Vol. 97, N° 1, pp. 27-41. <https://doi.org/10.1680/icien.1993.22378>
- Mair R.J., Wood D.M. (1987).** Pressuremeter testing: methods and interpretation. CIRIA Ground Engineering Report: In-situ testing, Butterworths, London, 160 pages.
- Masoud Z. Khan A.H. (2019).** An Improved Technique for Prebored Pressuremeter Tests. *KSCE Journal of Civil Engineering*. Technical Note. <https://doi.org/10.1007/s12205-019-1448-5>
- Ménard L. (1955).** Pressiomètre. Brevet d'invention N°. 1.117.983, 3 pages.
- Mestat Ph., Reiffsteck Ph. (2002).** Modules de déformation en mécanique des sols : définitions, détermination à partir des essais triaxiaux et incertitude. *Symp. Int. PARAM2002*, Paris, Presses de l'ENPC, pp. 393-400.
- Modoni G., Flora A., Mancuso C., Anh Dan L.Q., Koseki J., Balakrishnaiyer K., Tatsuoka F. (1999).** A simple experimental procedure for the complete characterization of small strain stiffness of gravels. *Pre-failure Deformation Characteristics of Geomaterials*, Rotterdam : Balkema, pp. 123-130.
- Oztoprak S, Bolton M.D. (2013).** Stiffness of sand through a laboratory test database. *Géotechnique* Vol. 63, N°. 1, pp. 54-70. <https://doi.org/10.1680/geot.10.P.078>
- Qiao T. (2011).** The Development, Design and Analysis of a New Centrifuge pressuremeter. Undergraduate thesis project, School of Civil & Resource Engineering, University of Western Australia, Australia.
- Rehman Z. (2010).** Development of a Pressuremeter to Operate in Alluvial Soils of Punjab. PhD thesis of doctor of philosophy, Departement of civil engineering, University of engineering and technology, Lahore, Pakistan, 212 pages.
- Reiffsteck Ph. (2002).** Nouvelles technologies d'essai en mécanique des sols-Etat de l'art. *Symposium International identification et détermination des paramètres des sols et des roches pour les calculs géotechniques PARAM 2002*, presses de l'ENPC / LCPC, Paris, pp. 201-242.
- Reiffsteck Ph., Reverdy G., Vincelas G., Sagnard N. (2005).** Pressiomètre autoforeur de nouvelle génération-PAF2000 *Symp. Int. ISP5-PRESSIO2005*, 50 ans de pressiomètres, Gambin et al. (eds.), vol. 1, Presses de l'ENPC/LCPC, pp. 113-126.
- Schnaid F. (2006).** Geo-characterisation and properties of natural soils by in situ tests. *Proceedings of the International Conference on Soil Mechanics and Geotechnical Engineering*, pp. 3-45. doi:10.3233/978-1-61499-656-9-3.

- Shaban A.M., Cosentino P.J. (2017).** Development of the Miniaturized Pressuremeter Test to Evaluate Unbound Pavement Layers. *Journal of Testing and Evaluation*, Vol.45, No.2, pp. 521–533. <https://doi.org/10.1520/JTE20150322>
- Stokoe K.H.I., Woods R.D. (1972).** In situ shear wave velocity by cross-hole method. *Journal of the Soil Mechanics and Foundations Division, ASCE*, 98(SM5), pp. 443–460.
- Tatsuoka F., Jardine R.J., Lo Presti D., Di Benedetto H. and Kodaka T. (1997).** Characterising the prefailure deformation properties of geomaterials. *Proceedings, 14th International Conference on Soil Mechanics and Foundation Engineering, Hamburg*, vol. 4, pp. 2129-2164.
- Thorel L., Gaudin C., Rault G., Garnier J., Favraud C. (2007).** A cone pressuremeter for soil characterisation in the centrifuge. *International Journal for Physical Modelling in Geotechnics* 7(1), pp. 25–32. <https://doi.org/10.1680/ijpimg.2007.070103>
- Vardanega P.J., Bolton M.D. (2013).** Stiffness of clays and silts: normalizing shear modulus and shear strain. *Journal of Geotechnical and Geoenvironmental Engineering*, Vol. 139, N°. 9, pp. 1575–1589. [https://doi.org/10.1061/\(ASCE\)GT.1943-5606.0000887](https://doi.org/10.1061/(ASCE)GT.1943-5606.0000887)
- Wang K., Xu G., Wang J., Wang C. (2018).** Self-boring in situ shear pressuremeter testing of clay from Dalian Bay, China. *Soils and Foundations*, Vol.58, N05, pp. 1212-1227. <https://doi.org/10.1016/j.sandf.2018.07.007>.
- Withers N.J., Schaap L.H.J., Dalton C.P. (1986).** The development of a full displacement pressuremeter. *International Symposium on Pressuremeter and its Marine Applications, Briaud et Audibert (Eds), ASTM STP 950, Texan*, pp. 38-56.
- Woods R.D. (1978).** Measurement of dynamic soil properties. In: *Proc. Earthquake Engineering and Soil Dynamics*, ASCE, New York, Vol. 1, pp. 91-78.
- Wroth C.P., Hughes J.M.O. (1972).** An instrument for the in situ measurement of the properties of soft clays. Report of departement of engineering, University of cambridge, CUED/C, Soils TR13, 29 pages.
- Zhang J., Andrus R.D., Juang C.H. (2005).** Normalized shear modulus and material damping ratio relationships. *Journal of Geotechnical and Geoenvironmental Engineering*, Vol. 131, N°. 4, pp. 453–464. [https://doi.org/10.1061/\(ASCE\)1090-0241\(2005\)131:4\(453\)](https://doi.org/10.1061/(ASCE)1090-0241(2005)131:4(453))

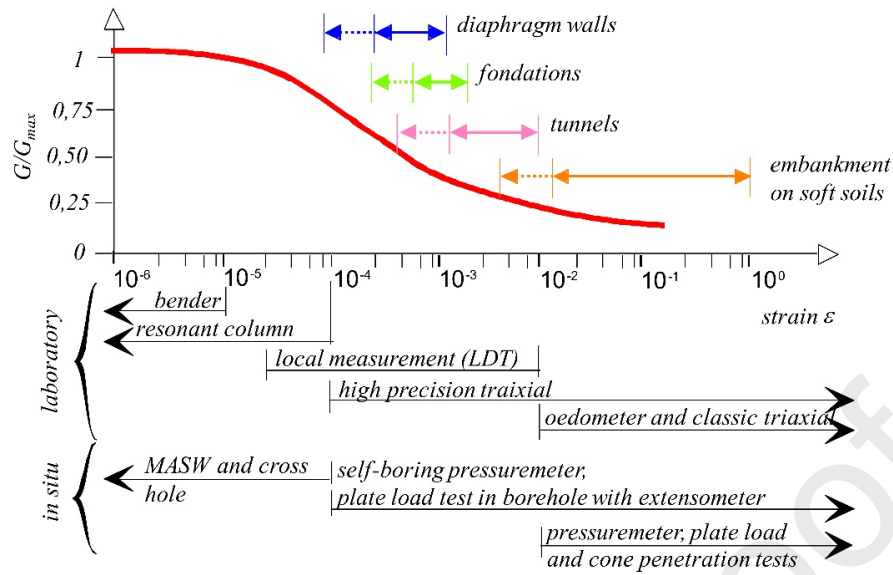


Fig. 1. Curve of reduction of the shear modulus with the strain for the different ranges of strains specific to the works and the tests of laboratory and in situ (Reiffsteck, 2002)

Table 1. Geometric characteristics of the probe.

		Notation	Value	Tolerance	
Flexible sheath probe	Central cell	Length (mm)	$l_s$	210	[0; +5]
		Outside diameter (mm)	$d_s$	58	[-2; +2]
	Guard cell	Length (mm)	$l_g$	120	[-15; +15]
		Outside diameter (mm)	$d_g$	58	[-2; +2]

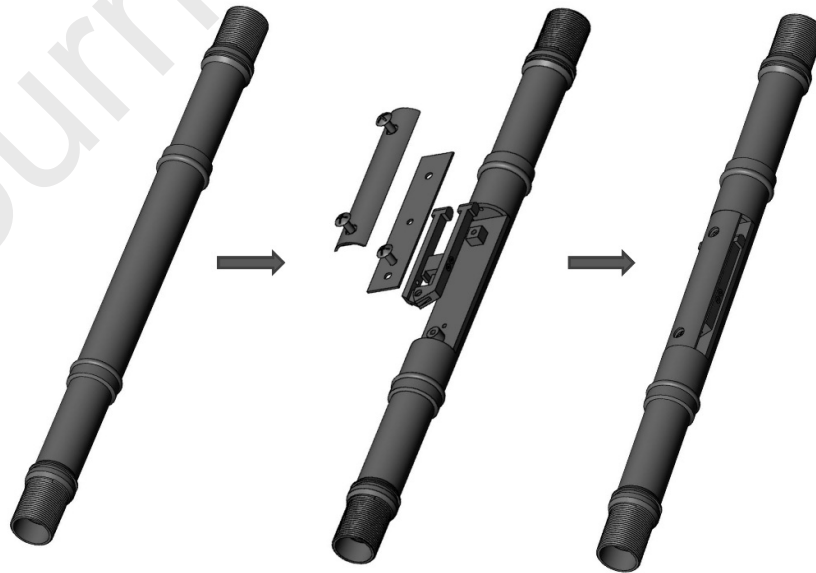
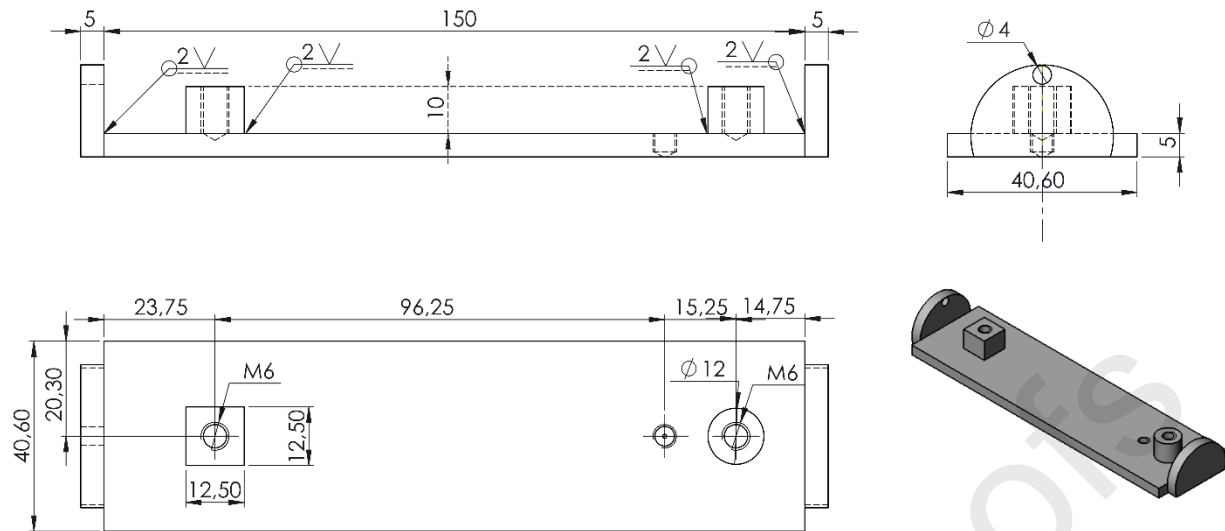
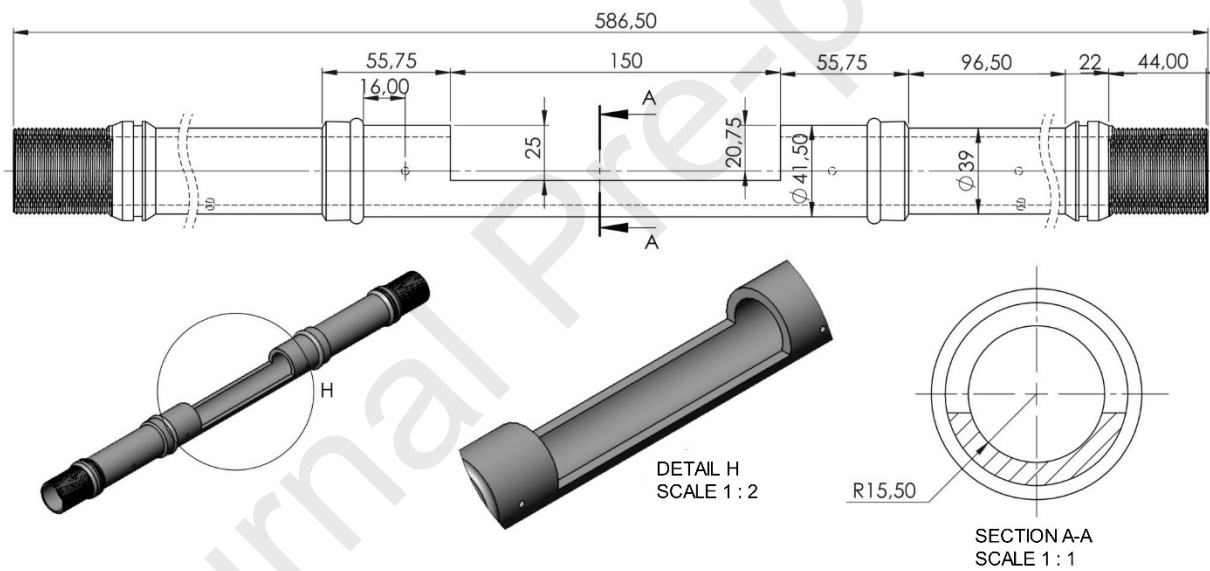


Fig. 2. Principle of the proposed model



**Fig. 3. The geometric characteristic of the test plate (the dimensions in mm)**



**Fig. 4. Illustration of the measurement area (the dimensions in mm)**



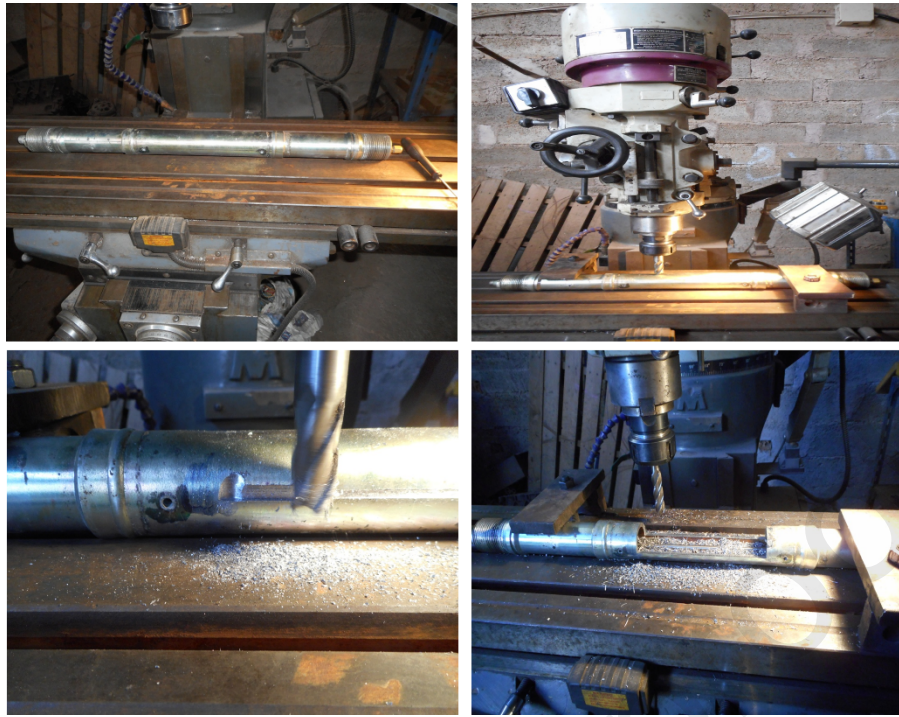


**Fig. 5. Real view of the creation of the measurement zone**

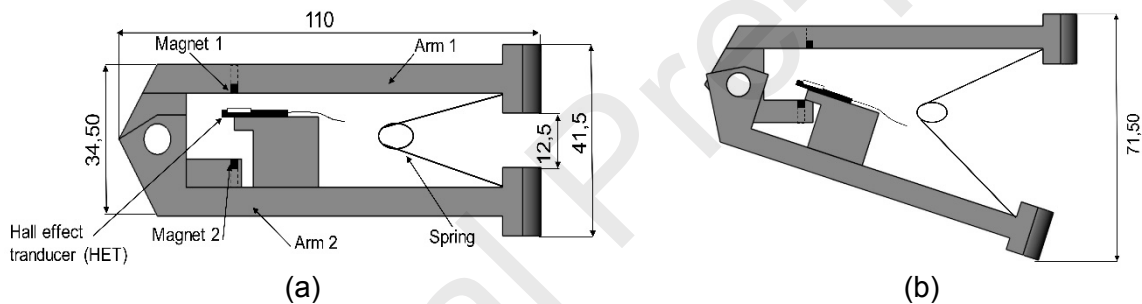


**Fig. 6. Measuring range of the feeler: a) Before expansion; b) After expansion**

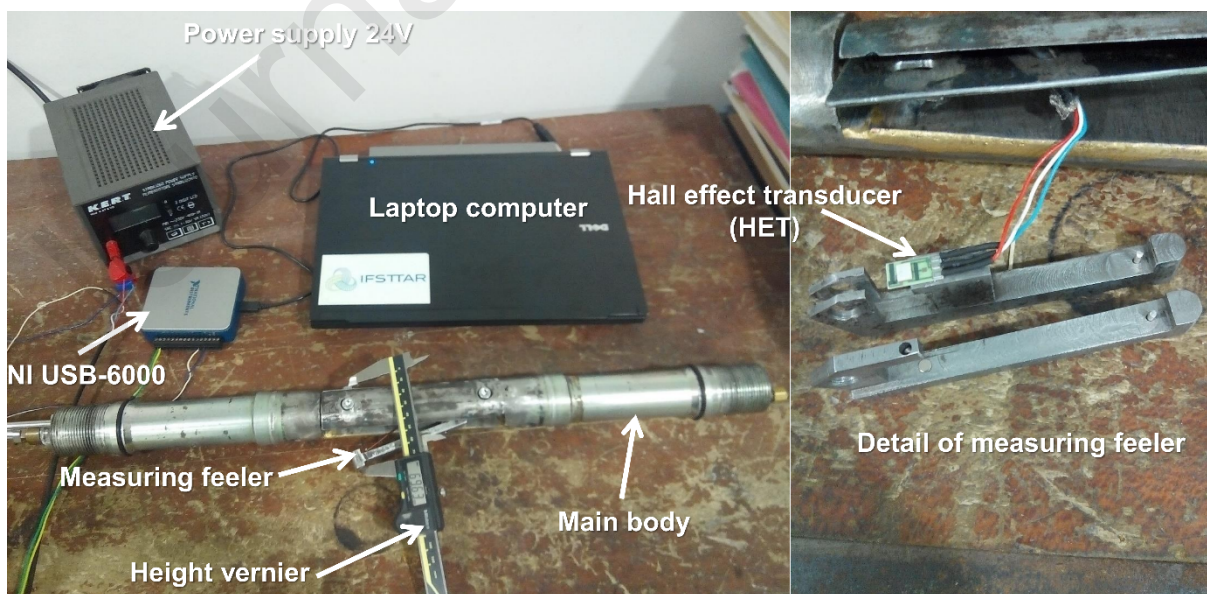


**Fig. 7. Assembly carried out for calibration**

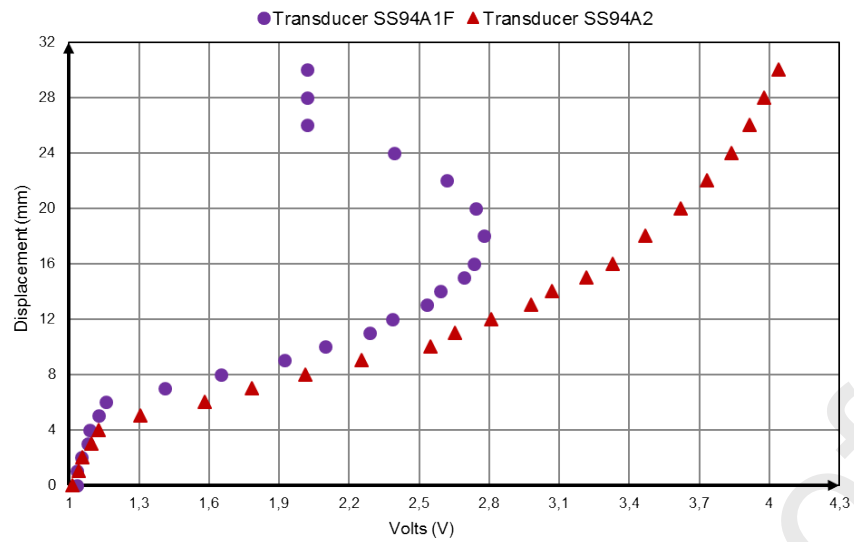


**Fig. 8. Effect of the SS94A1F and SS94A2 sensors on the measurement**

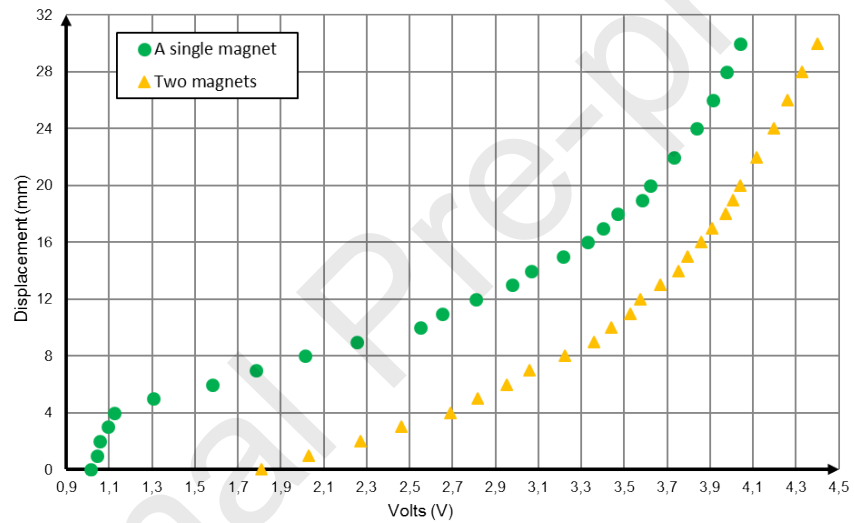


**Fig. 9. Influence of the magnetic polarization on the response of the sensor**



(a)



(b)

**Fig. 10. (a) KELLER pressure sensor used, (b) Digital regulator EV-6**



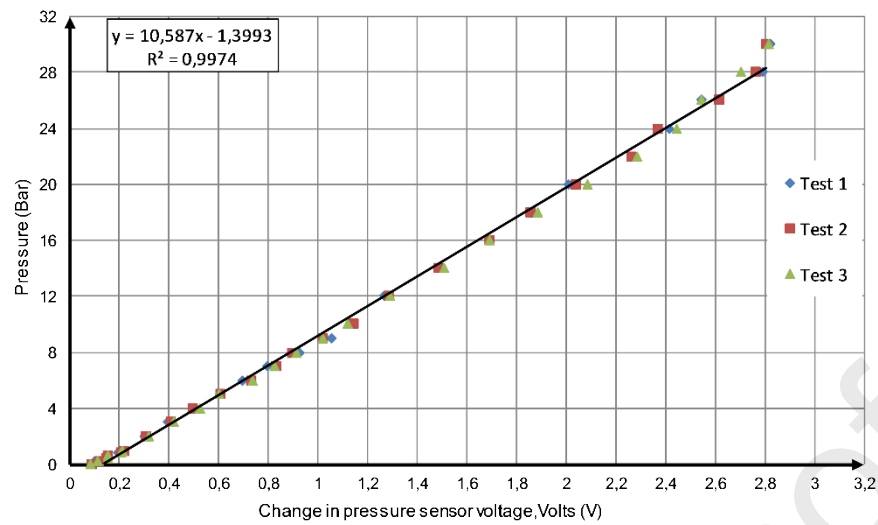


Fig. 11. Calibration curve of the pressure sensor

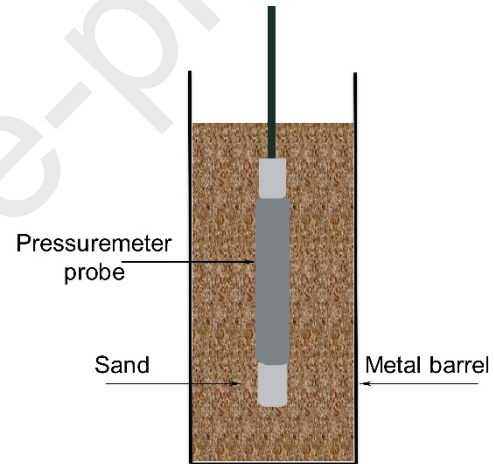


Fig. 12. General view of the workstation

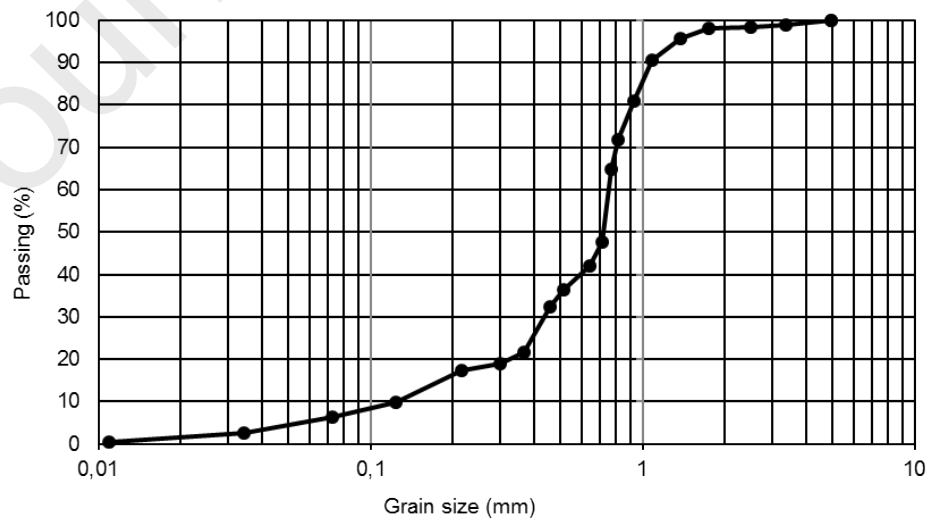


Fig. 13. Grain size distribution curve of tested sand

Table 2. Sand characteristics.

$D_{50}$ (mm)	$C_u$	$C_c$	$e_{min}$	$e_{max}$	$\rho_s$ (g/cm <sup>3</sup> )	$\rho_{dmin}$ (g/cm <sup>3</sup> )	$\rho_{max}$ (g/cm <sup>3</sup> )
0,71	6,33	1,17	0,423	0,568	2,65	1,690	1,861

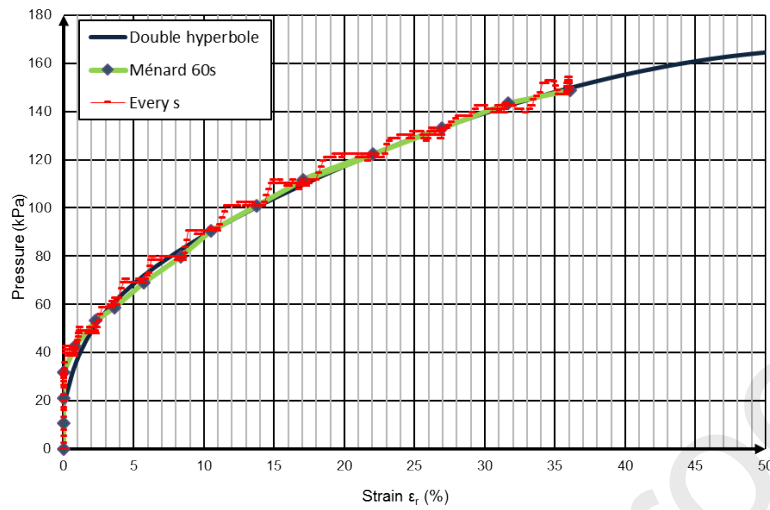


Fig. 14. Membrane calibration curve

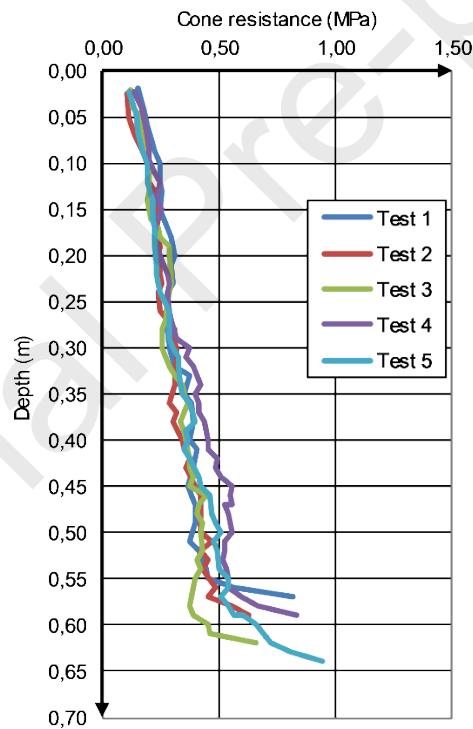
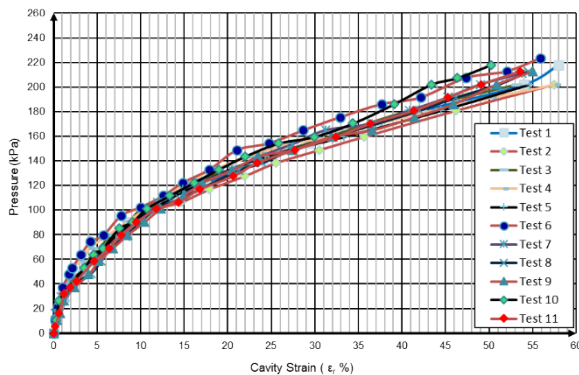
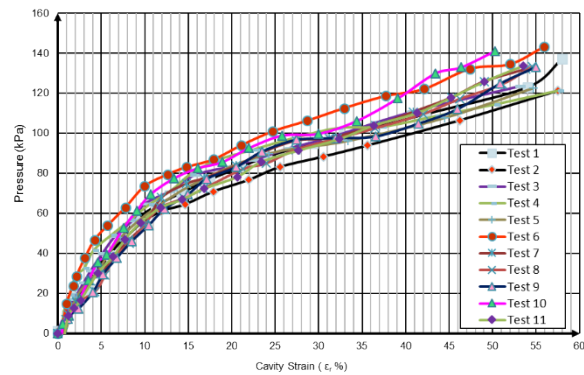


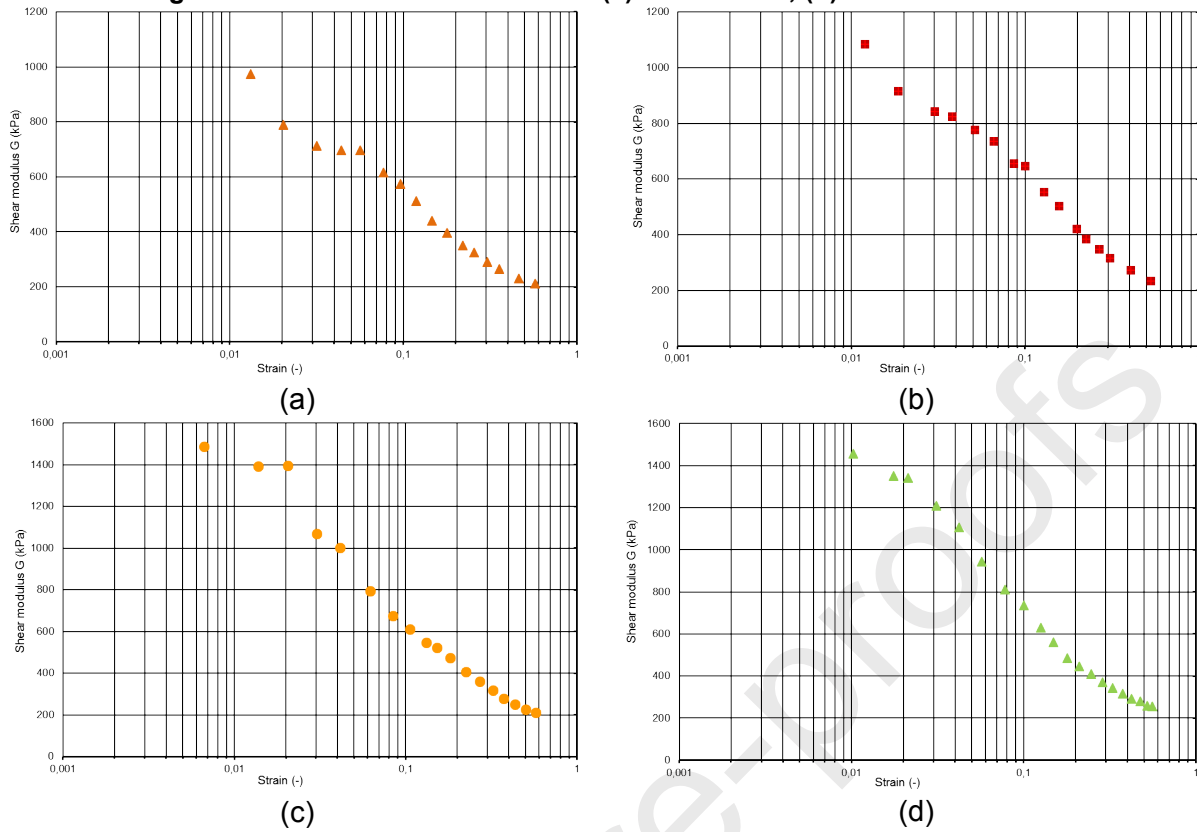
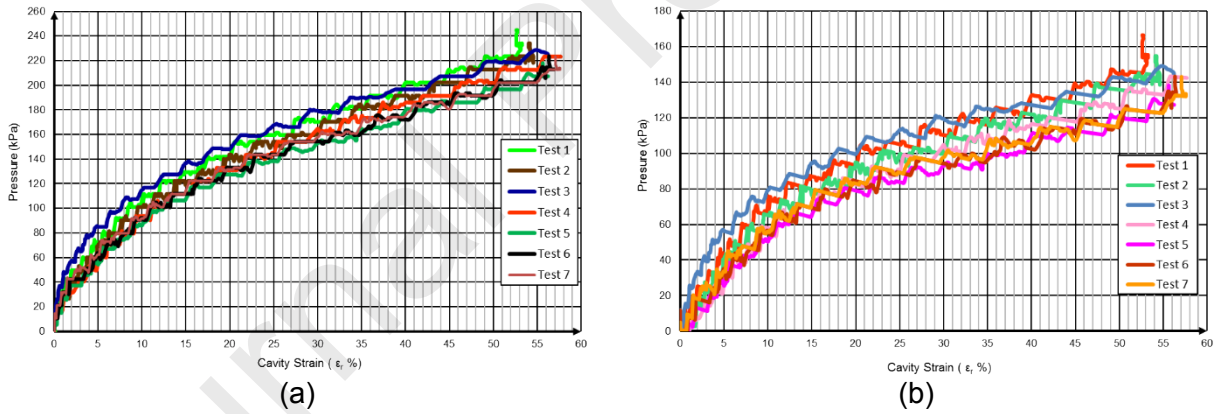
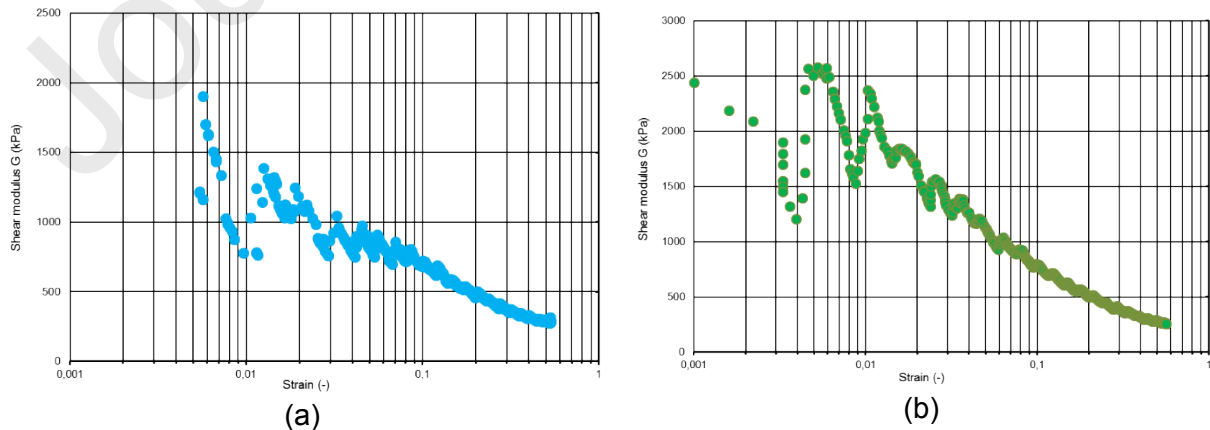
Fig. 15. Variation of dynamic resistance as a function of depth – loose sands

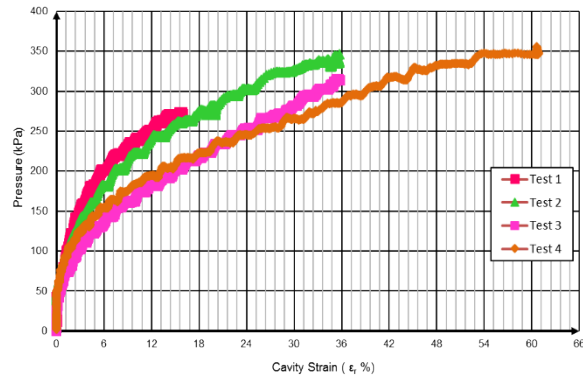


(a)

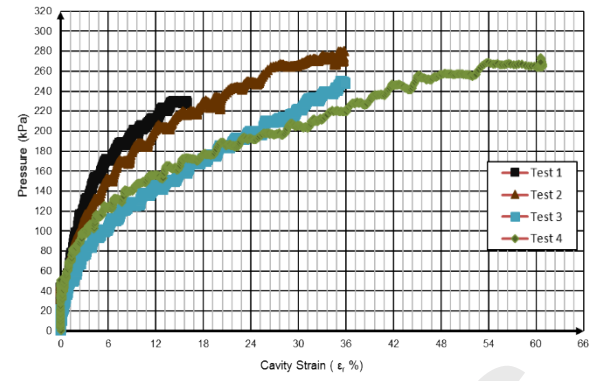


(b)

**Fig. 16. Results of monotonic tests. (a) raw curves.; (b) corrected curves****Fig. 17. Shear modulus Degradation. (a) Test 2 ; (b) Test 3, (c) Test 4 and (d) Test 6****Fig. 18. Results of the tests monotone loading proposed. (a) raw curves; (b) corrected curves****Fig. 19. Evolution of the shear moduli G with the cavity strain. (a) Test 1, (b) Test 3**

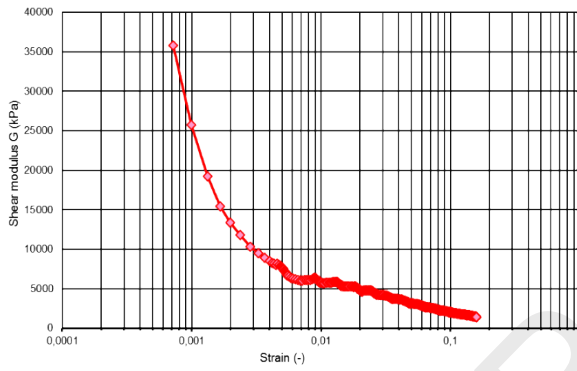


(a)

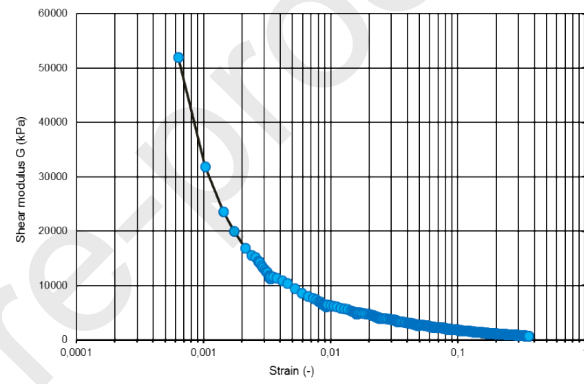


(b)

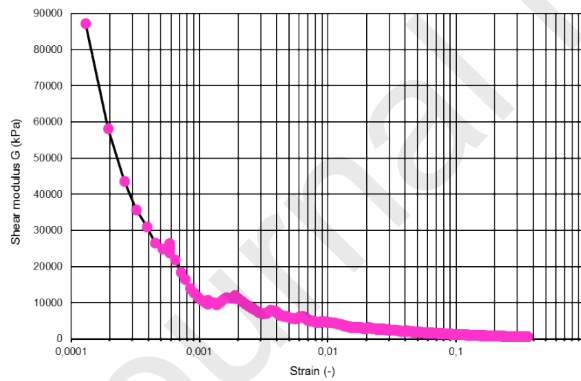
**Fig. 20. Results of monotonic tests on dense sand. (a) raw curves; (b) corrected curves**



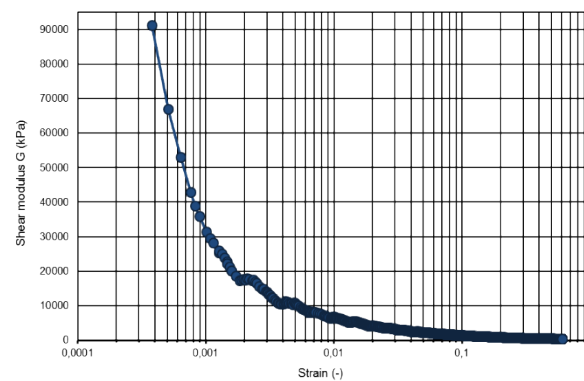
(a)



(b)



(c)



(d)

**Fig. 21. Shear Modulus Degradation. (a) Test 1, (b) Test 2, (c) Test 3 et (d) Test 4**

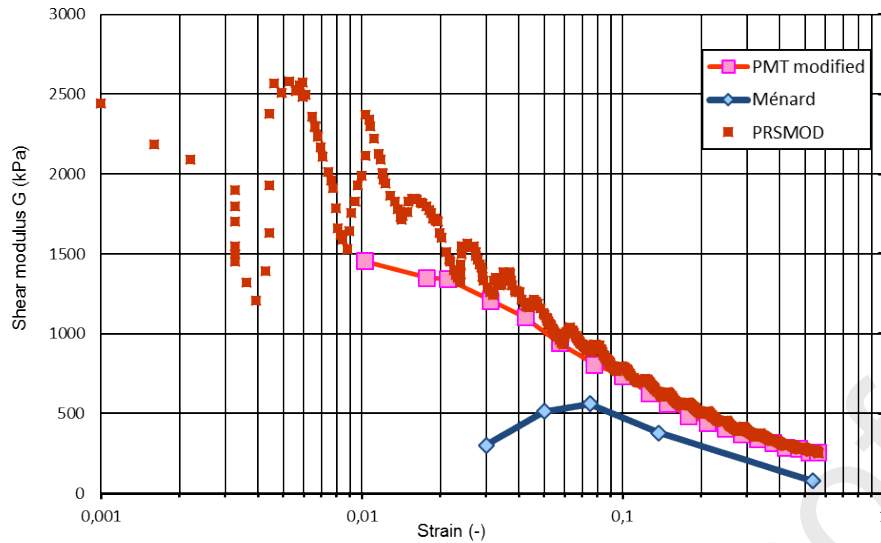


Fig. 22. Comparison between  $G$  determined by the modified probe and the Ménard probe

### Symbols and Abbreviations.

$l_s$	Length of the central cell.
$d_s$	Outside diameter of the central cell.
$l_g$	Length of the guard cell.
$d_g$	Outside diameter guard cell.
$p_c$	The corrected pressure
$p_r$	The raw pressure
$p_e$	Pressure due to the resistance of the membrane
$\sigma_{h0}$	The in-situ total horizontal stress
$G$	Shear modulus
$\varepsilon_r$	Radial strain.
$\Delta R$	Variation of the radius of the cavity.
$R_0$	Initial radius of the cavity.
$\Delta p$	Variation of the pressure
IFSTTAR	French institute of science and technology for transport, development and networks
LCPC	Central Laboratory of Bridges and Roads
$D_{50}$	mean grain size
$C_u$	coefficient of uniformity
$C_c$	coefficient of curvature
$e_{min}$	Minimum void index.
$e_{max}$	Maximum void index
$\rho_s$	Density of solid particles
$\rho_{dmin}$	Minimum dry density

$\rho_{dmax}$	Maximum dry density
PMT modified	Probe developed with loading according to the standard.
Ménard	Ménard probe with loading according to the standard.
PRSMOD	Probe developed with proposed loading.
PAF	New generation self-drilling pressuremeter
LDT	Local Deformation Transducer
LVDT	Linear Variable Differential Transformer



# **A New Protocol for Measuring Small Strains with a Pressuremeter Probe: Development, Design, and Initial Testing**

Soufyane AISSAOUI<sup>1</sup>, Abdeldjalil ZADJAOU<sup>2</sup>, Philippe REIFFSTECK<sup>3</sup>

<sup>1</sup>PhD Student, Department of Civil Engineering, Faculty of Technology, University Aboubekr BELKAID, Tlemcen, 22 rue Abi Ayed Abdelkrim, Fg Pasteur BP 119. 13000, Algeria. E-mail: aissaouisoufyane@yahoo.fr

<sup>2</sup>Professor, Department of Civil Engineering, Faculty of Technology, University Aboubekr BELKAID, Tlemcen, 22 rue Abi Ayed Abdelkrim, Fg Pasteur BP 119. 13000, Algeria. E-mail: a.zadjaoui@gmail.com

<sup>3</sup>Professor, Geotechnical Engineering, Environment, Natural Hazards and Earth Sciences Department, French Institute of Science and Technology for Transport, Development and Networks (IFSTTAR), University of Paris-Est, Champs sur Marne F-77447, Marne la Vallée Cedex 2, France. E-mail: philippe.reiffsteck@ifsttar.fr

## **Highlights**

- Development of a new pressuremeter apparatus equipped with a Hall Effect sensor.
- The new pressuremeter helps to have richer information concerning small strains.
- The device is different from the conventional by a deformation measurement system.
- Interpretation of results indicates mainly the degree of accuracy of the device.

**Declaration of interests**

☒ The authors declare that they have no known competing financial interests or personal relationships that could have appeared to influence the work reported in this paper.

☐ The authors declare the following financial interests/personal relationships which may be considered as potential competing interests:

--

# AUTHORSHIP STATEMENT

Manuscript title: **A New Protocol for Measuring Small Strains with a Pressuremeter Probe: Development, Design, and Initial Testing**

All persons who meet authorship criteria are listed as authors, and all authors certify that they have participated sufficiently in the work to take public responsibility for the content, including participation in the concept, design, analysis, writing, or revision of the manuscript. Furthermore, each author certifies that this material or similar material has not been and will not be submitted to or published in any other publication.

## 7. AUTHORSHIP CONTRIBUTIONS

### **Category 1**

Conception and design of study: S. Aissaoui, A. Zadjoui, Ph. Reiffsteck

acquisition of data: S. Aissaoui, A. Zadjoui, Ph. Reiffsteck

analysis and/or interpretation of data: S. Aissaoui, A. Zadjoui, Ph. Reiffsteck

### **Category 2**

Drafting the manuscript: S. Aissaoui, A. Zadjoui, Ph. Reiffsteck

revising the manuscript critically for important intellectual content: S. Aissaoui, A. Zadjoui, Ph. Reiffsteck

**Category 3**

Approval of the version of the manuscript to be published (the names of all authors must be listed):

S. Aissaoui, A. Zadjoui, Ph. Reiffsteck

**This statement is signed by all the authors** (*a photocopy of this form may be used if there are more than 10 authors*):

Author's name (typed)

Author's signature

Date

Soufyane AISSAOUIAISSAOUI02-09-2020Abdeldjalil ZADJAOUZADJAOU02-09-2020Philippe REIFFSTECKREIFFSTECK02-09-2020